Journal of Immunological Methods 474 (2019) 112647

Contents lists available at ScienceDirect

Journal of Immunological Methods

journal homepage: www.elsevier.com/locate/jim

Selection of potential cytokeratin-18 monoclonal antibodies following IGH repertoire evaluation in mice

Xinyang Li[a,b,c], Wei Zhang[b,c], Mi Huang[b,c], Zhe Ren[b,c], Chao Nie[a,b,c], Xiao Liu[b,c], Shuang Yang[b,c], Xiuqing Zhang[a,b,c], Naibo Yang[b,c,d,*]

[a] BGI Education Center, University of Chinese Academy of Sciences, Shenzhen 518083, China
[b] BGI-Shenzhen, Shenzhen 518083, China
[c] China National GeneBank, BGI-Shenzhen, Shenzhen 518120, China
[d] Complete Genomics, Inc., 2904 Orchard Parkway, San Jose, CA 95134, USA

ARTICLE INFO

Keywords:
CK18
Monoclonal antibody
IGH repertoire
Convergence

ABSTRACT

Cytokeratin 18 (CK18), the main scaffold protein of keratinocyte, is distributed in epithelial cells. This structural protein maintains the integrity and continuity of epithelial tissue. Cytokeratin is also frequently used as an immunohistochemical marker of tumor growth. In recent years, immune repertoire (IR) evaluation using next-generation sequencing (NGS) have become increasingly efficient. Here we deep sequenced the mouse IR of the immunoglobulin heavy chain (IGH) after CK18 immunization. We comprehensively analyzed the IR based on complementarity determining region 3 (CDR3) abundance, germline gene usage polarization, clone diversity, and lineage. We found many convergence characteristics after CK18 immunization. Convergence represents a phenomenon that antigen stimulation or pathogen exposure induces the antigen specific clone expansion and enrichment. The convergence could be used for the immune evaluation and antibody screen. After immunization, the IGHV5 gene clusters became preponderant. The abundance and length of the most frequent CDR3 both increased, nevertheless the IR diversity level decreased. From the convergent IGH repertoires, we selected and expressed six antibodies with the most frequent CDR3s and IGH V-J combinations. The ELISA results suggested all screened six antibodies bound CK18 specifically. The most potential antibody had 9.424E-10M M affinity for the interaction with the CK18. Therefore, this is the NGS platform has been first used for anti-CK18 monoclonal antibodies (MAbs) discovery. These analyses methods could also be used for vaccine evaluation.

1. Introduction

CK18 is the main scaffold protein of keratinocyte, produced by the intermediate filamentous filaments, that is distributed in most epithelial tissue cells (Chu and Weiss, 2002; Peduk et al., 2018). CK18 is associated with several important signaling pathways related to cell apoptosis, the cell cycle, and carcinogenesis (Peduk et al., 2018). As CK18 is often cleaved into many forms by caspase, this elevates the serum levels of its fragments (Sauer et al., 2018). The complete CK18 protein is also released into blood circulation during necrocytosis, while its cleaved fragments often enter the blood as a result of cell apoptosis. Thus, the circulating fragments of CK18 are often regarded as diagnostic markers for various diseases, including cancer (Peduk et al., 2018; Sauer et al., 2018). Monoclonal antibodies can be used to identify CK18 and its various fragments. Indeed, the serum concentrations of the M30 and M65 CK18 fragments have been shown to be useful diagnostic indicators of nasopharyngeal cancer (Sen et al., 2015). In addition, circulating caspase-cleaved CK18 levels are associated with mortality in patients with severe sepsis (Lorente et al., 2014). A recent clinical trial of chronic hepatitis B suggested that CK18-Asp396 was a highly-

Abbreviations: CDR3, complementarity determining region 3; CK18, cytokeratin 18; D50, diversity 50. It is positively related to diversity. It is the calculated percentage of dominant unique clones, accumulative reads of which made up for 50% of the total (ranges from 0 to 50 in theory); DNA, deoxyribonucleic acid; IgG, immunoglobulin gama; IgM, immunoglobulin mu; IGH, immunoglobulin heavy chain; IGHV, variable germline gene of the immunoglobulin heavy chain; IGHJ, joining germline gene of the immunoglobulin heavy chain; IMonitor, a robust pipeline for TCR and BCR repertoire analysis; IR, immune repertoire; J, joining germline gene; ka, binding rate (1/Ms); kd, dissociation rate (1/s); Kd, kd/ka, the affinity is measured in Kd; KD, kilo dalton; NGS, next-generation sequencing; nt, nucleotides; PBST, phosphate buffer solution with 0.05% tween-20; PCR, polymerase Chain Reaction; RACE, rapid amplification of cDNA end; RNA, ribonucleic acid; RU, response values; V, variable germline gene; V(D)J, variable, diversity and joining germline genes; V/J, variable and joining germline genes

* Corresponding author at: BGI-Shenzhen, Shenzhen 518083, China.
E-mail address: yangnaibo@genomics.cn (N. Yang).

https://doi.org/10.1016/j.jim.2019.112647
Received 17 May 2019; Received in revised form 12 July 2019; Accepted 13 August 2019
Available online 14 August 2019
0022-1759/

specific, independent biomarker of significant inflammation (Li et al., 2017).

Recently, NGS technology has developed quickly as costs have reduced. It allows more and more researchers could identify gene changes directly on a large scale (Shen et al., 2014). Unsurprisingly, NGS has been used to monitor human health conditions by analyzing the changes to the immune repertoires of clones (Cheng et al., 2018; Ghraichy et al., 2018). In 2014, Lu et al. reported the background repertoire of IgG antibodies in mice, providing the baseline IR before antigen immunization (Lu et al., 2014). If it were possible to summarize the characteristic molecular changes after antigen immunization, then, theoretically, IR sequencing data could be used directly to screen antibody sequences and to evaluate vaccines (Reddy et al., 2010).

As early as in 2010, bioinformatics analyses were used to evaluate and mine the antibody variable region (V)-gene repertoires of the bone marrow plasma cells of immunized mice (Reddy et al., 2010). In 2012, a proteomics approach combined with NGS technology was described, which identified human progesterone receptor A/B-specific antibody sequences directly from circulating polyclonal antibodies in the serum of an immunized mouse (Cheung et al., 2012). In addition, a molecular-level evaluation of the serum antibody repertoire after the seasonal influenza vaccination has recently been published (Lee et al., 2016). However, no studies focused on characterizing CK18-stimulated IRs.

Here, we aimed to combine NGS and bioinformatics analyses to evaluate the repertoire to screen anti-CK18 mAbs. As an initial proof of concept, we produced some specific antibodies could bind the CK18 antigen. We believe that our evaluation of CK18-stimulated IR will increase the ability to screen the CK18-specific antibody.

2. Methods and materials

2.1. Animals, immunization and ethics

We obtained six to eight-week-old specific pathogen free male BALB/c mice from Comparative Medicine Center of Yangzhou University. All of the mice were kept and immunized at the animal center of Vazyme Biotech Co., Ltd., Nanjing, China. One mouse was designated as CK18–1, and the other five mice were designated as CK18-2~6. The recombinant human CK18 antigen was provided by Professor Siqi Liu (BGI-Shenzhen, Shenzhen, China). We immunized each mouse with 50 μg of antigen in 250 μL phosphate buffered solution via subcutaneous injection for three times, once every other month (1st day, 31st day, and 61st day). Two weeks after the final immunization (75th day), all of the mice were killed and spleen lymphocytes were harvested. Spleen sampling was performed according to a humane and ethical protocol reviewed and approved by the Bioethics and Biological Safety Review Committee of BGI-Shenzhen (building 11, beishan industrial zone, yantian district, Shenzhen, China). The permit number was FT 15052. All animal experiments comply with the ARRIVE guidelines and were carried out in accordance with the U.K. Animals (Scientific Procedures) Act, 1986 and associated guidelines, EU Directive 2010/63/EU for animal experiments.

2.2. IGH repertoire construction and sequencing

We constructed six IGH repertoires. Total RNA was extracted from approximately 1E + 07 mononuclear spleen cells using an RNEasy kit (Qiagen, Hilden, Germany) following the manufacturer's protocol. We used N6 random primers and the reverse transcriptase SSII (Invitrogen, Carlsbad, CA, USA) to produce cDNA templates from 8 μg total RNA. 5'-RACE (rapid amplification of cDNA end) was used to amplify mouse immunoglobulin genes from the cDNA. Meanwhile, the mouse IGH primers, which annealed at the first constant region, were designed and synthesized (IgG1/2-primer: CAGGGGCCAGTGGATAGA-3; IgG3-primer: CAGATGGGGCTGTTGTTGTA; and IgM-primer: AAGACATTTG GGAAGGACTGA). The ~500 bp PCR products were separated using 2% agarose gel electrophoresis, and purified using a Qiagen gel-purification kit (Qiagen, Hilden, Germany) following the manufacturer's protocol. Purified PCR products were then tagged with 8-bp barcodes for cluster identification. Final products were sequenced with Mi-Seq (illumina, San Diego, CA, USA), using a 2 × 300-bp paired-end read strategy.

2.3. Bioinformatics analysis and evaluation of the IGH repertoire

The IGH repertoire sequences were analyzed with IMonitor (Zhang et al., 2015; Li et al., 2016). Briefly, we checked sequence quality, removed low quality reads, and merged cleaned paired-end reads. The merged reads were searched against V and J germline sequences from the international ImMunoGeneTics information system (IMGT; http://www.imgt.org/) using BLAST (Li et al., 2016). We then realigned each result, and selected the best V/J alignment for each merged read. We next performed the following analyses: CDR3 analysis, germline gene usage polarization, clone diversity, and lineage analysis.

CDR3 is critical for interactions with antigens; the length, abundance, and diversity of this sub region directly affect the entire immune system (Kitaura et al., 2017; Liu et al., 2017; Rettig et al., 2018). Antigen stimulation, infection and disease intensify the germline gene usage polarizations as part of the immune response (Wu et al., 2016; Liu et al., 2017). Thus, the identification of V/J gene usage polarizations might improve screening for specific antibodies and vaccine evaluations.

Diversity is an essential character of the IR and high diversity is important for a healthy immune system (Georgiou et al., 2014; Hou et al., 2016; Madi et al., 2017). IR diversity is mainly generated during lymphocyte development by V(D)J recombination, random insertions and deletions, and systemic mutations (Carlson et al., 2013; Fu et al., 2017). Here, we used the number of unique CDR3s (Madi et al., 2017) and the D50 value (Hou et al., 2016) to evaluate IR diversity (positively related). Many sequences have the same CDR3 and each type of CDR3 has ≥1 sequencing reads. So the unique CDR3 number represents the CDR3 type or the variety of CDR3 clonotypes in the IR. D50 is the calculated percentage of dominant unique clones, accumulative reads of which made up for 50% of the total (ranges from 0 to 50 in theory). Lineage size and number are also associated with IR diversity.

2.4. Antibody expression and ELISA assay

We screened the most probable CK18-specific sequences. After codon optimization and gene synthesis, the mother plasmid pFUSE-CHIg-MG1 (InvivoGen, HongKong, China) was used to construct expression vector. Separately, previous study reported a germline IG kapa light chain gene (Accession NO. AJ231205) highly expressed in non-immunized mice (Aoki-Ota et al., 2012). It was selected and synthesized to co-expressed with these IGH clones. Mammalian cells (human embryonic kidney 293F) were co-transfected with two vectors of heavy and light chains (1:1) combination using ExpiFectamine™ 293 Transfection Kit. Cells were harvested at approximately five days post-transfection and assayed for recombinant protein expression. The antibody proteins were purified with the 1 mL Protein G column (GE Healthcare, USA). The SDS-PAGE gel electrophoresis was used to detect the whole Ab integrity.

Antigen-antibody binding was detected by ELISA assay. Briefly, the CK18 antigens were coated on the 96 wells plate, 200 ng/well and incubated overnight at 4 °C. After blocking with 3% BSA for 2 h at 37 °C, three gradient concentrations of these recombinant antibodies were added into each well with the PBS as blank control, and with blank serum as the negative controls for 1 h at 37 °C. After washing with phosphate buffer solution with 0.05% tween-20 (PBST), 100 μL horseradish peroxidase -conjugated anti-mouse IgG antibodies were added into each well at 37 °C for 45 min. After washing, 100 μL TMB was added into each well and the plate was incubated in the dark at 37 °C for 10 min. The reaction was stopped by 50 μL of 1 M sulfuric acid. The

absorbance at 450 nm was measured by a microplate reader (Bio-Rad).

2.5. Affinity determination

CK18The affinity of the recombinant Abs for CK18 was detected by the Biacore T200 Protein Interaction System (GE Healthcare). Recombinant CK18 antibody was captured on a Protein A chip. CK18-Ab was then diluted to 6 μg/mL in PBST and injected at 10 μ L/min for 25 s. Finally, it led to a capture level of approximately ~600 response units (RU) of Ab.

The affinity value of recombinant Ab was determined by injecting 6 concentrations of CK18 antigen, in triplicate, with a running buffer of PBST. CK18 antigens were injected at 30 μL/min for 240 s followed by a 300 s dissociation time. Between injections, residual bound protein was eliminated by regeneration with 100 mM glycine solution, pH 2.75, running at 30 μL/min for 20s. Binding sensor grams from these injections were processed and analyzed using the Biacore evaluation software. Binding curves were fit to the data with a Langmuir model, using grouped on rate, off rate and R_{max} values.

2.6. Statistical analysis

The mouse germline genes were derived from the IMGT database using IMGT/HighV-QUEST, which determines the most likely germline derivations of the V and J germline genes (Giudicelli et al., 2017). The relative frequency of each observed germline subgroup was calculated based on the alignment results. Statistical significance was tested using Student's paired *t*-test. $P < .05$ was considered as statistically significant.

3. Results

3.1. NGS data description

Raw sequencing data was basically processed using the software "IMonitor"(Zhang et al., 2015). Mi-Seq pair-end sequencing yielded an average of 1,032,423 raw reads per sample (Table S1). After removing adapter contamination and low quality reads (i.e., reads that were more than > 5% "N"), ~75.56% of the reads per sample were retained. Baseline repertoire data for unimmunized mice have previously been published (Lu et al., 2014).All the sequencing data could be acquired from the Nucleotide Sequence Archive of China National Gene Bank by two project numbers CNP0000103 and CNP0000593 (https://db.cngb.org/cnsa/).

3.2. CDR3 analysis

The top 100 CDR3s made up less of the total CDR3s in the CK18–1/2 mice (47%) and it made up half in the CK18–5/6 mice (50% and 51%), as compared to the CK18–3/4 mice (57% and 55%; Fig. 1). Thus, the predominant clones in the CK18–3/4 mice converged, consistent with a previous study (Jackson et al., 2014). This implies that the frequency of some specific clones increased continuously after antigen stimulation (Parameswaran et al., 2013). The most abundant CDR3 of the third and fourth mice reflected this phenomenon (CK18–3: 11.58%; CK18–4: 13.38%; Fig. S1).

The CDR3 lengths in each mouse were unevenly distributed (Fig. 2; (Waltari et al., 2018)). In CK18-1 mouse, 24.54% of all CDR3s were 36 nucleotides (nt) long, while in CK18-2/4/5, 21.56%/36.75%/27.22% of all CDR3s were 45 nt long, and in CK18-3, 17.63% of all CDR3s were 42 nt long, and in CK18–6, 24.50% of all CDR3s were 39 nt long; This was inconsistent with the baseline IGH repertoire (15.8% of all CDR3s were 36 nt long (Lu et al., 2014)), indicating that immunization may increase the length and frequency of the most common CDR3s. This mechanism may facilitate the antibody response to antigen stimulation. It suggested that some CK18-specific antibody clones may had long CDR3 length and high frequency.

3.3. IGHV-J gene usage analysis

In unimmunized mice, the IGHV1 family germline and the IGHV5 gene cluster were the most frequently used (Lu et al., 2014). Here, the IGHV5 family dominated the V gene usage histogram for all of the CK18 immunized mice as well (Fig. 3). However, IGHV3–2-02 was no longer the dominant germline gene in the CK18 immunized mice. Instead, the use of the subtype gene IGHV5–17 was significantly greater, as compared to the unimmunized mice (an increase from ~10% to > 20%; $P < .05$).

As to the IGHJ genes, Fig. S2 shows the relative usage frequencies of all the IGHJ germline genes. Clearly, except for CK18–6, the usage of IGHJ1 genes usage do not have the dominant degree (< 16%). Except for CK18–5, the IGHJ2 or IGHJ4 germline gene still had the dominant usage frequencies (> 30%). There were no significant differences in IGHJ gene usage between the CK18-immunized mice and the unimmunized mice. It is important to note that the IGHJ4 of the CK18–4 mouse had enjoyed the dominance (> 48%).

Each CK18-immunized mouse exhibited a particular dominant VJ combination (Fig. 4). Notably, in the CK18–4 mouse, the IGHV5–17/IGHJ4 pair had the highest frequency (29.98%), as like in the CK18–3/

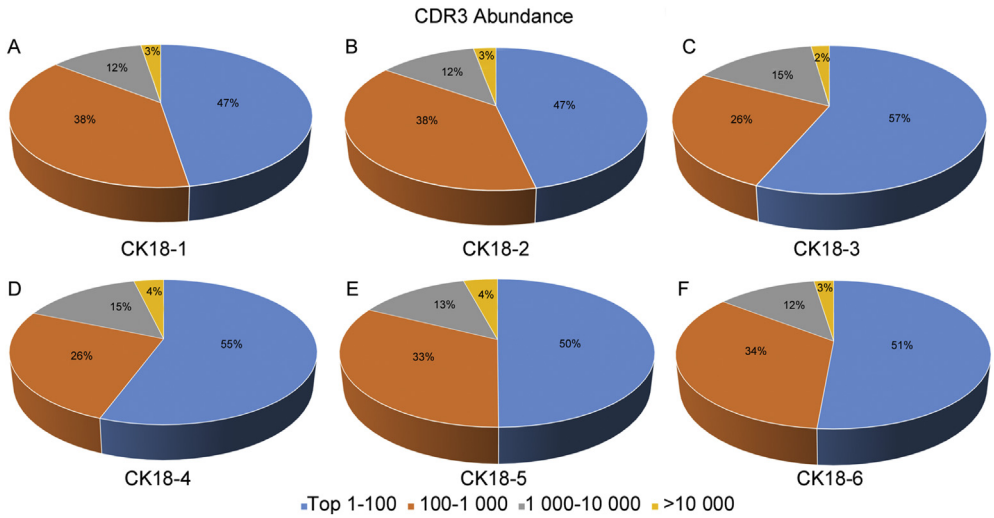

Fig. 1. Relative CDR3 abundance across six mice tested. It is divided into four groups by CDR3 abundance: Top 1–100; 100–1000; 1000–10,000; > 10,000.

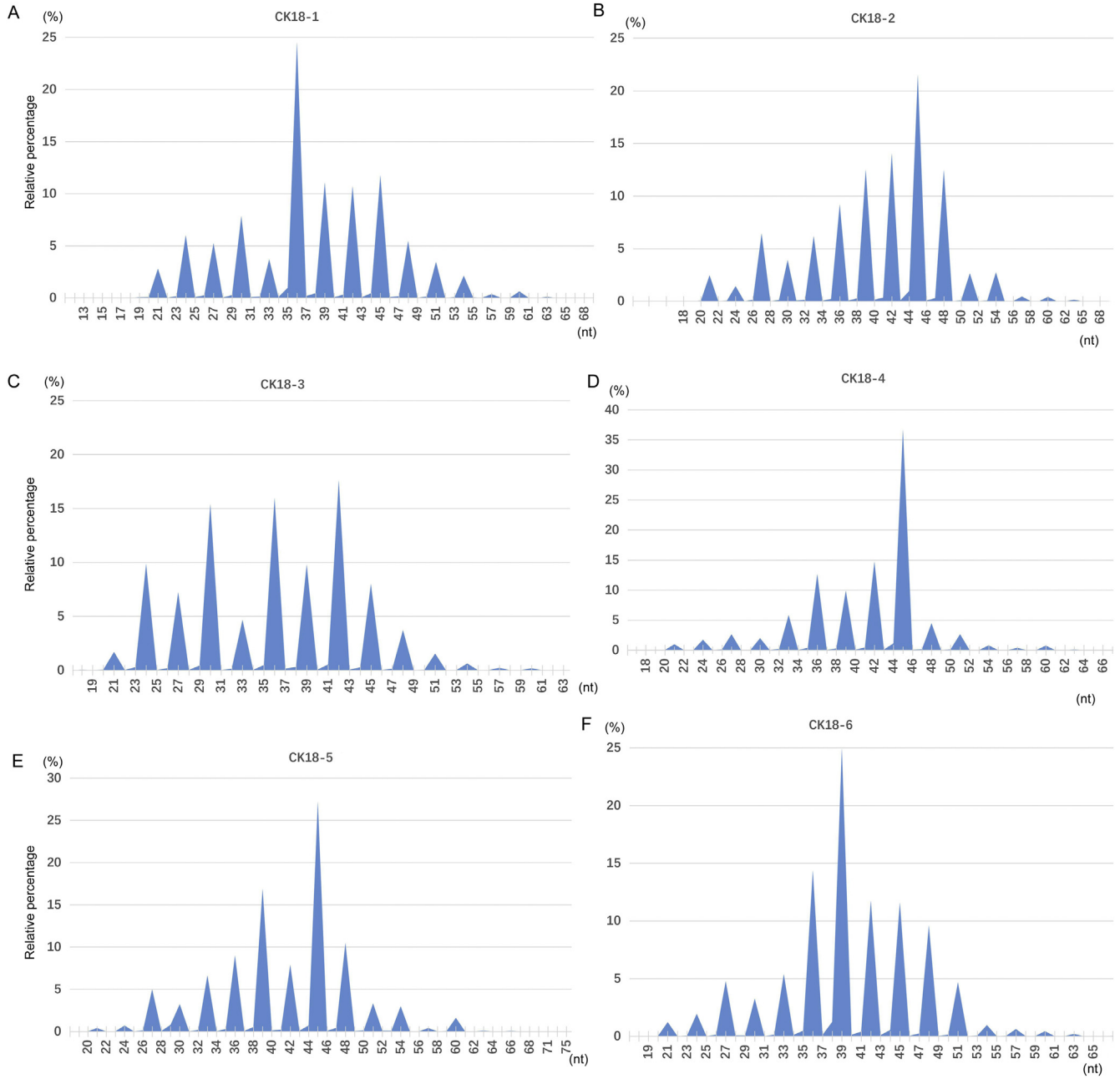

Fig. 2. Relative frequency of CDR3 as a function of length (in nucleotides, nt) in the six mice tested. The x-axes represent the nucleotides length of the most CDR3s; the y-axes represent the relative frequency.

5/6 mice. The CK18–4 mouse also had the most VJ pairings (Fig. S3). This indicated that the IR of mouse CK18–4 was converging after CK18 immunization. This was consistent with the above-mentioned data showing that the predominant clones of immunized animals tend to converge (Parameswaran et al., 2013; Jackson et al., 2014). It suggested that some CK18-specific clones may be characterized by the IGHV5–17/IGHJ4 pairing usage.

3.4. Diversity evaluation

Sufficient IR diversity is crucial for a powerful adaptive immune system (Gearhart, 2002; Hou et al., 2016). We evaluated the diversity of the IGH repertoires in the six mice after immunization based on the number of unique CDR3s. We found that the CK18-4 mouse had the most unique CDR3s across all six of the mice, and the CK18-3 mouse had the fewest (Fig. 5).

We also evaluated IR diversity based on the D50. Our results indicated that the CK18–1 mouse had the highest level diversity based on D50, even though this mouse did not have the most unique CDR3s (Fig. 5). The CK18–4 mouse also had the lowest IR diversity based on D50. This suggested that the response of the CK18–4 mouse to immunization was strongest convergent, which is consistent with our other results.

3.5. Lineage analysis

To comprehensively evaluate the immune responses of the mice after the CK18 immunization, a clone lineage analysis was performed (Fig. 6). A lineage represents that all its sequences originated from the same ancestral B cell. In this study, it refers to the sequences that were originated from the same VDJ recombination with no or one amino acid difference in the CDR3 (Jiang et al., 2013). Each bubble represents a

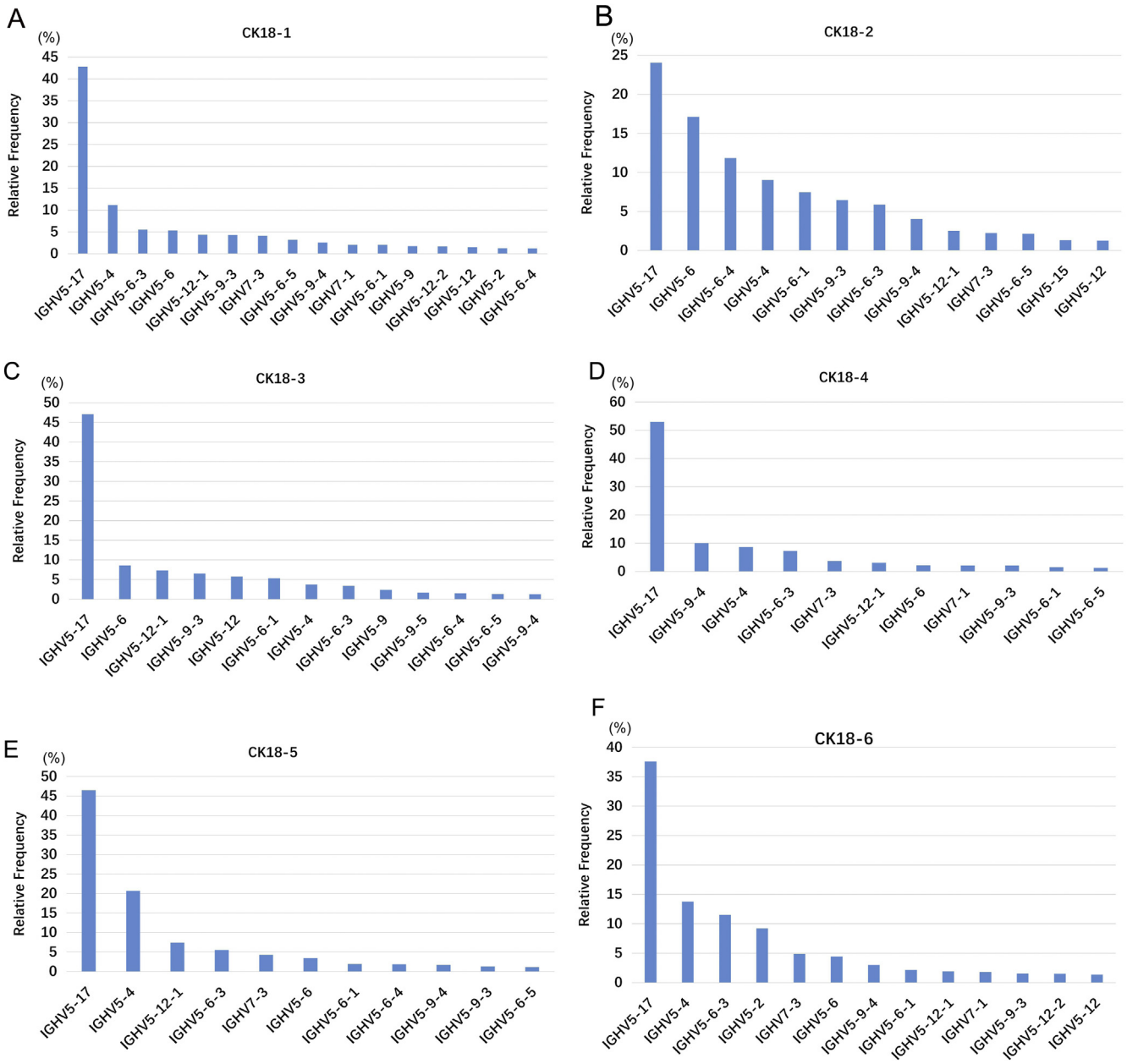

Fig. 3. IGHV gene usages across the six mice. All of the V gene subtypes with relative usage frequencies ≥1% are given on the x-axes; the y-axes represent the relative frequency.

lineage. The bubble size reflects lineage magnitude. We found that the lineage diagram of the CK18-4 mouse was obviously different from that of the others. In contrast, the largest lineage of CK18-4 had > 25,000 unique nt sequences. The largest lineages of the other mice had only < 15,000 unique nt sequences (Fig. 6). This indicated that many novel changes appeared after stimulation with the CK18 antigen for the CK18-4 mouse. Thus, more nucleotide sequences newly appeared in the CK18-4 had the same CDR3 sequences, further supporting convergence. It suggested that the CK18-specific clones could be screened in the novel large lineage.

3.6. SDS-PAGE, ELISA and Affinity determination

Based on the above immune evaluation, we screened one IGH clone from each mouse respectively. These clones were characterized by the most frequently CDR3 and most frequently VJ combination in each mouse. Besides, these clones are in their respective largest lineages. The SDS-PAGE gel results showed that these antibodies were correctly expressed (reduced: heavy chain ~50KD, and light chain~25KD, Fig. 7A; Non-reduced: 150KD, Fig. 7B).

ELISA results (Fig. 7C) showed that compared with the PBS and negative controls, all six screened antibodies bound to the CK18 antigen specifically. Especially for the CK18-4-Ab, its OD450 value did not reduce on three different dilutions (10μg, 5μg and 2.5μg). It showed that CK18-4-Ab has highest specificity and binding efficiency with CK18 antigen among all six Abs.

Furthermore, the affinity between the Abs and CK18 antigen were detected by the surface plasmon resonance technology. The curves in Fig. 7D showed that the CK18-4-Ab/CK18 had a fast binding rate (ka = 1.077E+5 1/Ms) and a slow dissociation rate (kd = 1.015E-4 1/s). The built-in evaluation software showed that the CK18-4-Ab had a 9.424E-10 M affinity (Kd) with the CK18 antigen after the curve automatic fitting. The CK18-3-Ab had a 1E-07 M affinity (Kd), and the others had fast dissociation rates (kd ≥ 1E-03 1/s; Kd ≥ 1E-07 M; data

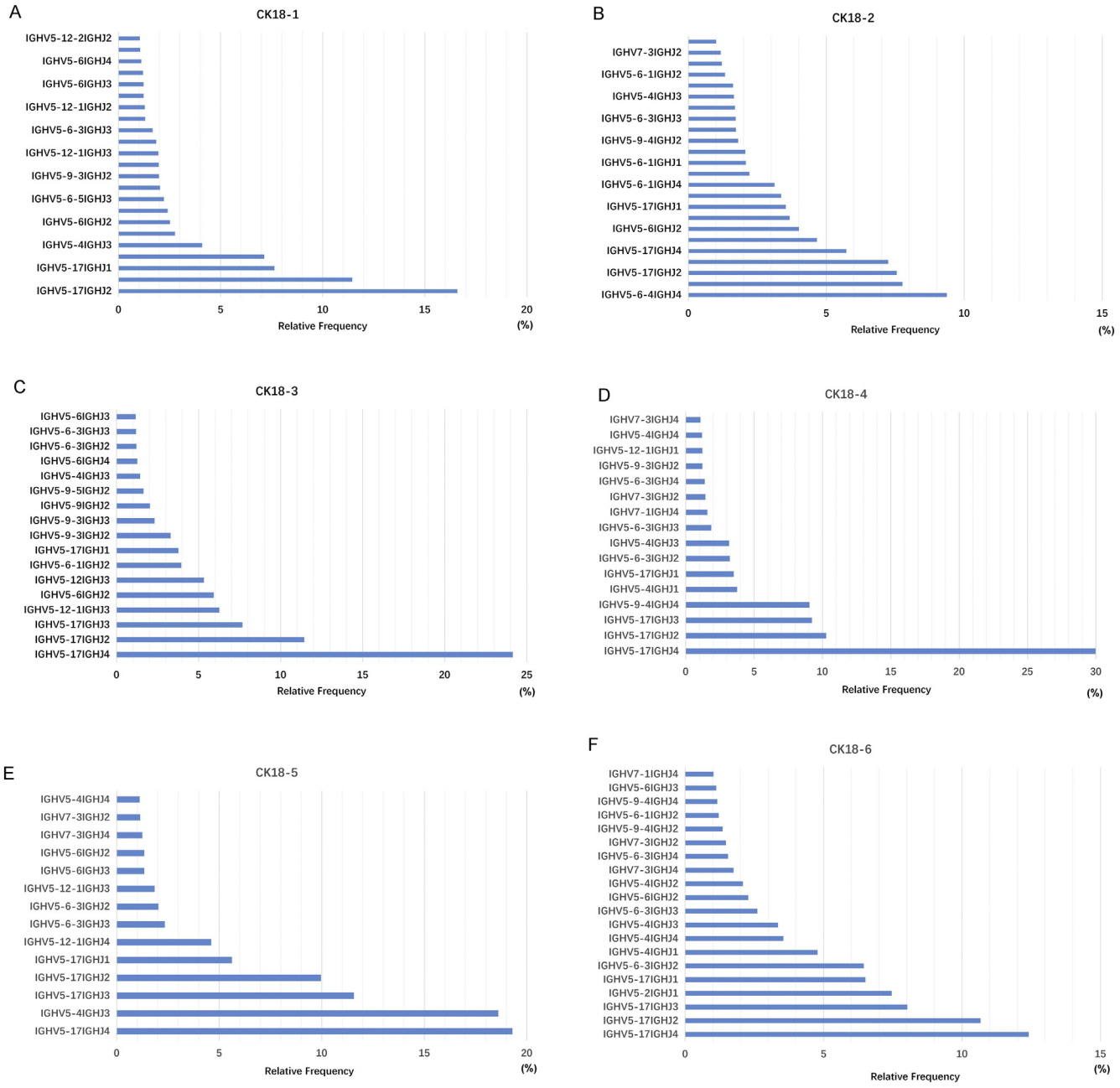

Fig. 4. IGHV-J gene combination frequency across the six mice. The x-axes represent the relative frequency. All of the V-J pairing with relative usage frequencies ≥1% are given on the y-axes.

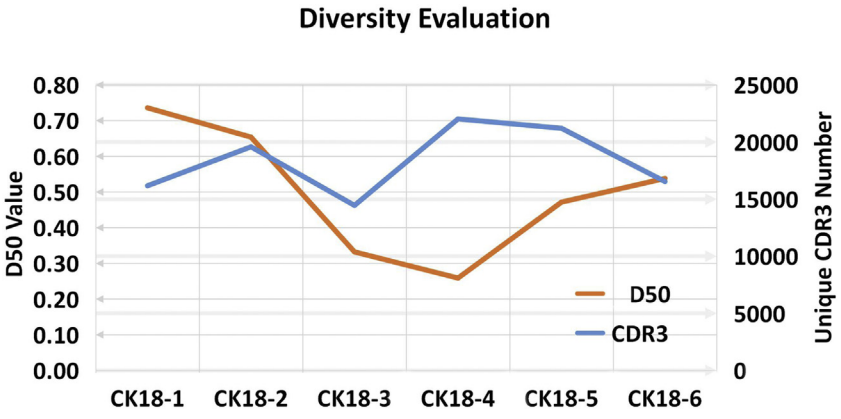

Fig. 5. Diversity evaluation. Evaluation of IR diversity in six mice based on two different metrics: number of unique CDR3s (blue line), and D50 (brown line). The x-axis represents the six mice; The right y-axis represents the number of unique CDR3s (big arrows). The left y-axis represents the D50 value (small arrows). The D50 value of a given repertoire is positively correlated to diversity (theoretical range: 0–50; (Hou et al., 2016). (For interpretation of the references to colour in this figure legend, the reader is referred to the web version of this article.)

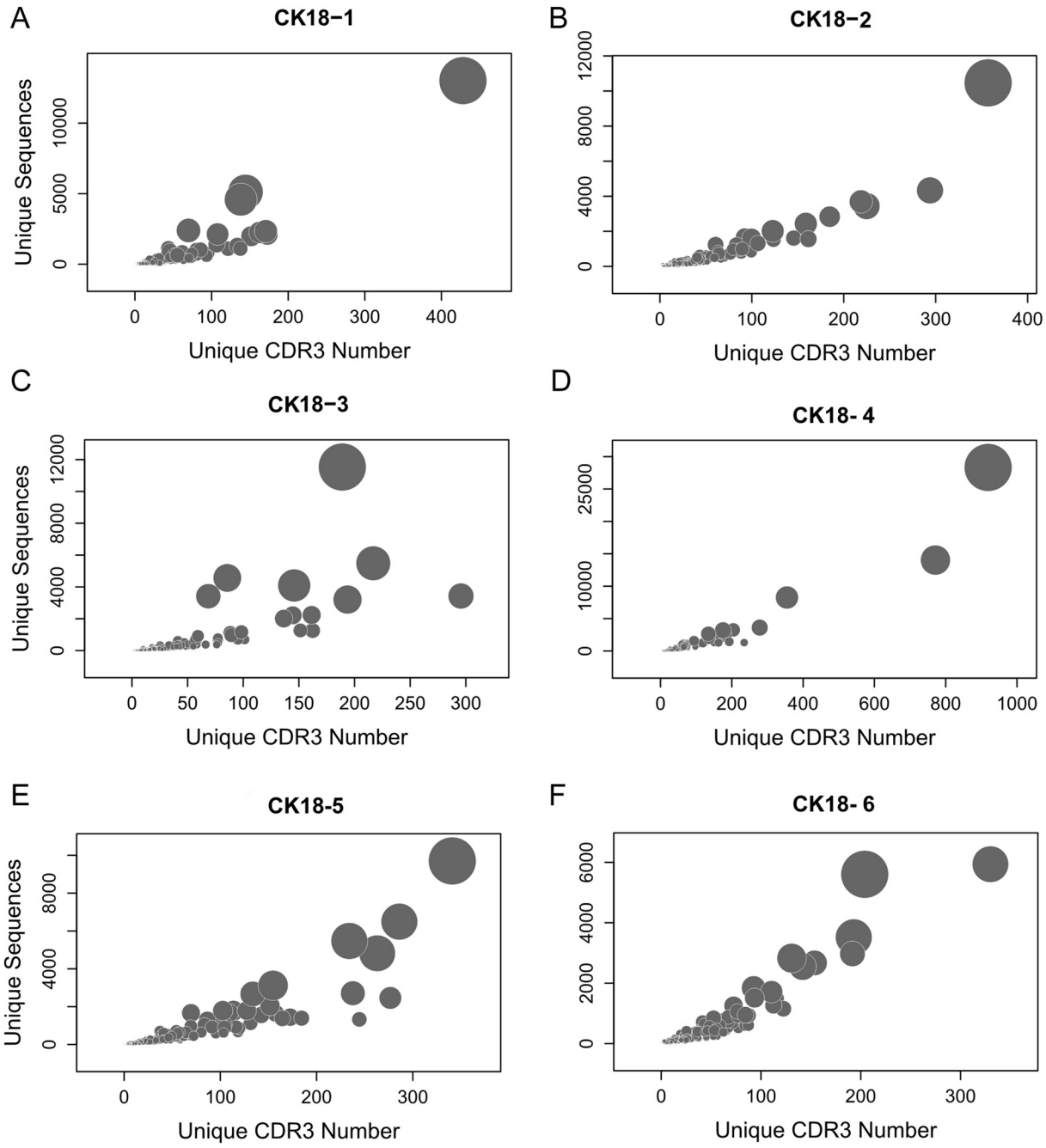

Fig. 6. Lineage analysis bubble map of the six mice. Each bubble represents a lineage; bubble size reflects lineage magnitude. For each bubble (lineage), the x-axes represent the numbers of the corresponding unique CDR3s and the y-axes represent the number of corresponding unique nucleotide sequences.

not shown). However, with high specificity, they are appropriate for the diagnostic reagent development.

4. Discussion

Many previous studies reported that CK18 and its fragments are biomarkers suitable for improving prediction and diagnosis of suspected diseases such as acute intestinal graft versus host disease and many types of cancers (Li et al., 2017; Peduk et al., 2018; Sauer et al., 2018). The diagnosed antibody is needed. Antibody repertoire sequencing by NGS is a valuable tool for antibody discovery.

IR characteristics after immunization are associated with antigen-specific immune clones (Lavinder et al., 2014). These IR characters include germline gene usage polarization, CDR3 changes, and IR diversity. Here, we evaluated the stimulated IGH repertoire. After immunization, these mice IRs showed different levels of convergences, which could be used to evaluate the level of the immune response to immunization (positively related). The more convergent the IR becomes, the stronger the immune response is and the more probable efficient antibody we screened. On diversity evaluation, D50 is normalized to be a calculated percentage of dominant unique clones, accumulative 50% total reads. So D50 value (Hou et al., 2016) is more objective than the unique CDR3 number.

Heavy-light chain natural pairing is an important factor for a high affinity antibody. In recent years, microdroplet embedding and single B cell sequencing technology facilitates the heavy and light chain simultaneous sequencing (DeKosky et al., 2015). However, emulsion embedding and single cell sequencing need complex operating

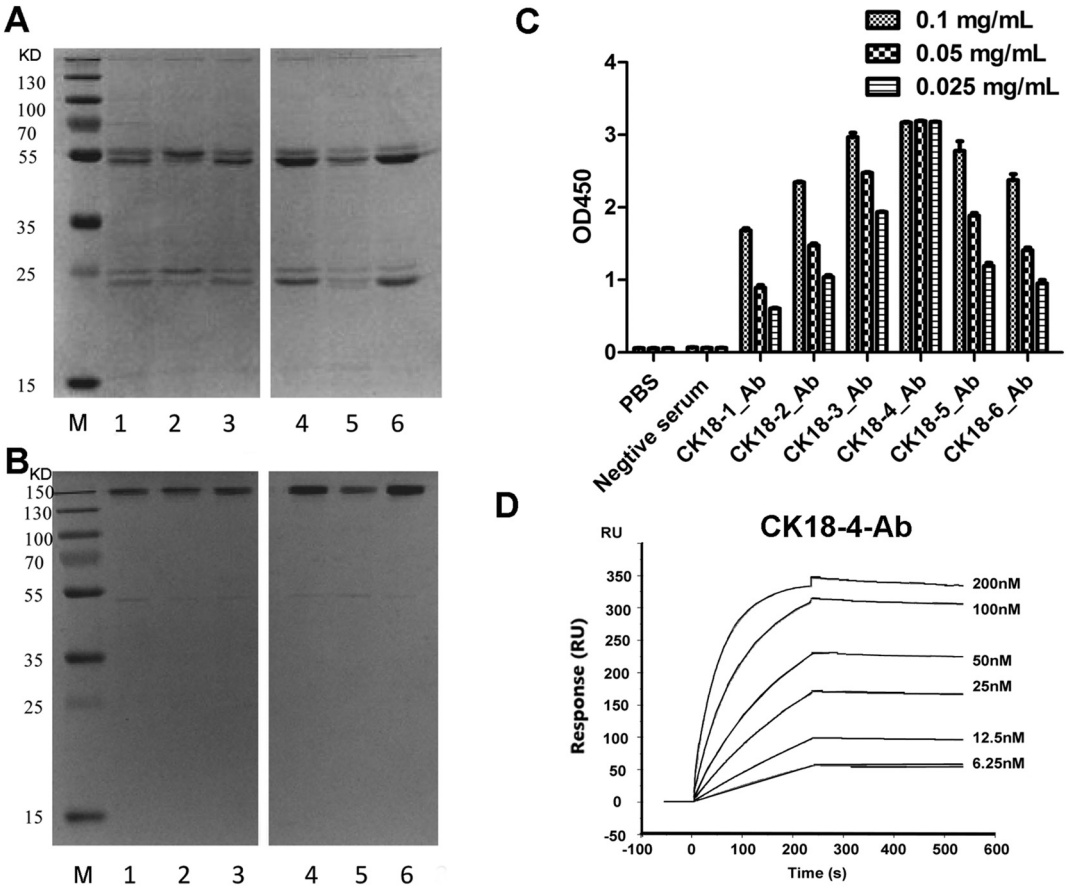

Fig. 7. Protein expression and affinity determination. A. The reduced SDS-PAGE gel results of the six Abs. B. The non-reduced SDS-PAGE gel results of the six Abs. "M" represents the protein molecular weight marker (kilo Dalton, KD). "1 ~ 6" represents the CK18–1–6 Abs. C. The ELISA results of the six Abs reacted with the CK18 antigen. The x-axis represents the different controls and six Abs. The y-axis represents the OD450 value. D. The affinity determination results of the CK18–4-Ab interacted with the CK18 antigen on the flow cells. The different lines represent different injection concentrations. The x-axis represents the timeline (s). The y-axis represents the relative response value (RU) of the antibody-antigen interaction. ka: binding rate (1/Ms); kd: slow dissociation rate (1/s); Kd: kd/ka, the affinity is measured in Kd.

procedures, and it is also very expensive. As demonstrated in previous analysis, the germline light chains can functionally pair with a variety of heavy chains (Gray et al., 2016). We selected a high expressed germline light gene to co-express the six whole Abs successfully. Besides, previous reports suggested that phylogenetic pairing of heavy-light chain can provide a means to approximate natural pairing (Zhu et al., 2013). In the early stage of the NGS-based Ab discovery, the predicted pairing methods are easier and more cost-effective.

PCR and sequencing errors are known problems that affect IR sequencing (Georgiou et al., 2014). To reduce these errors, we performed PCR and sequencing error correction with IMonitor. After correction, the mean error rate across all of the sequences and the percent of error-bearing sequences decreased significantly (Zhang et al., 2015).

In this study, we evaluated CK18-elicited IGH repertoires and analyzed the characteristics of the immune clones. We had screened six antigen-specific antibodies and they could be utilized to develop diagnose reagent with high affinity and specificity. Furthermore, these bioinformatics analyses can be readily applied to vaccine evaluation and Ab discovery.

Funding

This study was supported by P.R.China, MST Special Fund (Project Name: Single cell sequencing based antibody discovery). We also thank the funding support from Science, Technology and Innovation Commission of Shenzhen Municipality under grant NO. JSGG20170412153009953 and NO. JCY20170817145305022).

Supplementary data to this article can be found online at https://doi.org/10.1016/j.jim.2019.112647.

Declaration of Competing Interest

The authors declare that they have no competing interests.

Acknowledgments

We thank Dr. Bo Tang and Vazyme Biotech Co., Ltd. for the supports on sample collection.

References

Aoki-Ota, M., Torkamani, A., Ota, T., Schork, N., Nemazee, D., 2012. Skewed primary Igkappa repertoire and V-J joining in C57BL/6 mice: implications for recombination accessibility and receptor editing. J. Immunol. 188, 2305–2315.

Carlson, C.S., Emerson, R.O., Sherwood, A.M., Desmarais, C., Chung, M.-W., Parsons, J.M., Steen, M.S., LaMadrid-Herrmannsfeldt, M.A., Williamson, D.W., Livingston, R.J., Wu, D., Wood, B.L., Rieder, M.J., Robins, H., 2013. Using synthetic templates to design an unbiased multiplex PCR assay. Nat. Commun. 4, 2680.

Cheng, C., Wang, B., Gao, L., Liu, J., Chen, X., Huang, H., Zhao, Z., 2018. Next generation sequencing reveals changes of the gammadelta T cell receptor repertoires in patients with pulmonary tuberculosis. Sci. Rep. 8, 3956.

Cheung, W.C., Beausoleil, S.A., Zhang, X., Sato, S., Schieferl, S.M., Wieler, J.S., Beaudet, J.G., Ramenani, R.K., Popova, L., Comb, M.J., Rush, J., Polakiewicz, R.D., 2012. A proteomics approach for the identification and cloning of monoclonal antibodies from serum. Nat. Biotechnol. 30, 447–452.

Chu, P.G., Weiss, L.M., 2002. Keratin expression in human tissues and neoplasms. Histopathology 40, 403–439.

DeKosky, B.J., Kojima, T., Rodin, A., Charab, W., Ippolito, G.C., Ellington, A.D., Georgiou, G., 2015. In-depth determination and analysis of the human paired heavy- and light-chain antibody repertoire. Nat. Med. 21, 86–91.

Fu, L., Li, X., Zhang, W., Wang, C., Wu, J., Yang, H., Wang, J., Liu, X., 2017. A comprehensive profiling of T- and B-lymphocyte receptor repertoires from a Chinese-origin rhesus macaque by high-throughput sequencing. PLoS One 12, e0182733.

Gearhart, P.J., 2002. The roots of antibody diversity. Nature 419, 29.

Georgiou, G., Ippolito, G.C., Beausang, J., Busse, C.E., Wardemann, H., Quake, S.R., 2014. The promise and challenge of high-throughput sequencing of the antibody repertoire. Nat. Biotechnol. 32, 158–168.

Ghraichy, M., Galson, J.D., Kelly, D.F., Truck, J., 2018. B-cell receptor repertoire sequencing in patients with primary immunodeficiency: a review. Immunology 153, 145–160.

Giudicelli, V., Duroux, P., Kossida, S., Lefranc, M.-P., 2017. IG and TR single chain fragment variable (scFv) sequence analysis: a new advanced functionality of IMGT/V-QUEST and IMGT/HighV-QUEST. BMC Immunol. 18, 35.

Gray, S.A., Moore, M., VandenEkart, E.J., Roque, R.P., Bowen, R.A., Van Hoeven, N., Wiley, S.R., Clegg, C.H., 2016. Selection of therapeutic H5N1 monoclonal antibodies following IgVH repertoire analysis in mice. Antivir. Res. 131, 100–108.

Hou, D., Ying, T., Wang, L., Chen, C., Lu, S., Wang, Q., Seeley, E., Xu, J., Xi, X., Li, T., Liu, J., Tang, X., Zhang, Z., Zhou, J., Bai, C., Wang, C., Byrne-Steele, M., Qu, J., Han, J., Song, Y., 2016. Immune repertoire diversity correlated with mortality in avian influenza a (H7N9) virus infected patients. Sci. Rep. 6, 33843.

Jackson, K.J., Liu, Y., Roskin, K.M., Glanville, J., Hoh, R.A., Seo, K., Marshall, E.L., Gurley, T.C., Moody, M.A., Haynes, B.F., Walter, E.B., Liao, H.X., Albrecht, R.A., Garcia-Sastre, A., Chaparro-Riggers, J., Rajpal, A., Pons, J., Simen, B.B., Hanczaruk, B., Dekker, C.L., Laserson, J., Koller, D., Davis, M.M., Fire, A.Z., Boyd, S.D., 2014. Human responses to influenza vaccination show seroconversion signatures and convergent antibody rearrangements. Cell Host Microbe 16, 105–114.

Jiang, N., He, J., Weinstein, J.A., Penland, L., Sasaki, S., He, X.S., Dekker, C.L., Zheng, N.Y., Huang, M., Sullivan, M., Wilson, P.C., Greenberg, H.B., Davis, M.M., Fisher, D.S., Quake, S.R., 2013. Lineage structure of the human antibody repertoire in response to influenza vaccination. Sci. Transl. Med. 5, 171ra19.

Kitaura, K., Yamashita, H., Ayabe, H., Shini, T., Matsutani, T., Suzuki, R., 2017. Different somatic Hypermutation levels among antibody subclasses disclosed by a new next-generation sequencing-based antibody repertoire analysis. Front. Immunol. 8, 389.

Lavinder, J.J., Wine, Y., Giesecke, C., Ippolito, G.C., Horton, A.P., Lungu, O.I., Hoi, K.H., DeKosky, B.J., Murrin, E.M., Wirth, M.M., Ellington, A.D., Dorner, T., Marcotte, E.M., Boutz, D.R., Georgiou, G., 2014. Identification and characterization of the constituent human serum antibodies elicited by vaccination. Proc. Natl. Acad. Sci. U. S. A. 111, 2259–2264.

Lee, J., Boutz, D.R., Chromikova, V., Joyce, M.G., Vollmers, C., Leung, K., Horton, A.P., DeKosky, B.J., Lee, C.H., Lavinder, J.J., Murrin, E.M., Chrysostomou, C., Hoi, K.H., Tsybovsky, Y., Thomas, P.V., Druz, A., Zhang, B., Zhang, Y., Wang, L., Kong, W.P., Park, D., Popova, L.I., Dekker, C.L., Davis, M.M., Carter, C.E., Ross, T.M., Ellington, A.D., Wilson, P.C., Marcotte, E.M., Mascola, J.R., Ippolito, G.C., Krammer, F., Quake, S.R., Kwong, P.D., Georgiou, G., 2016. Molecular-level analysis of the serum antibody repertoire in young adults before and after seasonal influenza vaccination. Nat. Med. 22, 1456–1464.

Li, X., Duan, X., Yang, K., Zhang, W., Zhang, C., Fu, L., Ren, Z., Wang, C., Wu, J., Lu, R., Ye, Y., He, M., Nie, C., Yang, N., Wang, J., Yang, H., Liu, X., Tan, W., 2016. Comparative analysis of immune repertoires between Bactrian Camel's conventional and heavy-chain antibodies. PLoS One 11, e0161801.

Li, J., Verhaar, A.P., Pan, Q., de Knegt, R.J., Peppelenbosch, M.P., 2017. Serum levels of caspase-cleaved cytokeratin 18 (CK18-Asp396) predict severity of liver disease in chronic hepatitis B. Clin. Exp. Gastroenterol. 10, 203–209.

Liu, S., Hou, X.L., Sui, W.G., Lu, Q.J., Hu, Y.L., Dai, Y., 2017. Direct measurement of B-cell receptor repertoire's composition and variation in systemic lupus erythematosus. Genes Immun. 18, 22.

Lorente, L., Martin, M.M., Gonzalez-Rivero, A.F., Ferreres, J., Sole-Violan, J., Labarta, L., Diaz, C., Jimenez, A., Borreguero-Leon, J.M., 2014. Serum levels of caspase-cleaved cytokeratin-18 and mortality are associated in severe septic patients: pilot study. PLoS One 9, e109618.

Lu, J., Panavas, T., Thys, K., Aerssens, J., Naso, M., Fisher, J., Rycyzyn, M., Sweet, R.W., 2014. IgG variable region and VH CDR3 diversity in unimmunized mice analyzed by massively parallel sequencing. Mol. Immunol. 57, 274–283.

Madi, A., Poran, A., Shifrut, E., Reich-Zeliger, S., Greenstein, E., Zaretsky, I., Arnon, T., Laethem, F.V., Singer, A., Lu, J., Sun, P.D., Cohen, I.R., Friedman, N., 2017. T cell receptor repertoires of mice and humans are clustered in similarity networks around conserved public CDR3 sequences. eLife 6, e22057.

Parameswaran, P., Liu, Y., Roskin, K.M., Jackson, K.K., Dixit, V.P., Lee, J.Y., Artiles, K.L., Zompi, S., Vargas, M.J., Simen, B.B., Hanczaruk, B., McGowan, K.R., Tariq, M.A., Pourmand, N., Koller, D., Balmaseda, A., Boyd, S.D., Harris, E., Fire, A.Z., 2013. Convergent antibody signatures in human dengue. Cell Host Microbe 13, 691–700.

Peduk, S., Tatar, C., Dincer, M., Ozer, B., Kocakusak, A., Citlak, G., Akinci, M., Tuzun, I.S., 2018. The role of serum CK18, TIMP1, and MMP-9 levels in predicting R0 resection in patients with gastric cancer. Dis. Markers 2018, 5604702.

Reddy, S.T., Ge, X., Miklos, A.E., Hughes, R.A., Kang, S.H., Hoi, K.H., Chrysostomou, C., Hunicke-Smith, S.P., Iverson, B.L., Tucker, P.W., Ellington, A.D., Georgiou, G., 2010. Monoclonal antibodies isolated without screening by analyzing the variable-gene repertoire of plasma cells. Nat. Biotechnol. 28, 965–969.

Rettig, T.A., Ward, C., Bye, B.A., Pecaut, M.J., Chapes, S.K., 2018. Characterization of the naive murine antibody repertoire using unamplified high-throughput sequencing. PLoS One 13, e0190982.

Sauer, S., Hüsing, J., Hajda, J., Neumann, F., Radujkovic, A., Ho, A.D., Dreger, P., Luft, T., 2018. A prospective study on serum cytokeratin (CK)-18 and CK18 fragments as biomarkers of acute hepato-intestinal GVHD. Leukemia 32, 2685–2692.

Sen, F., Yildiz, I., Odabas, H., Tambas, M., Kilic, L., Karadeniz, A., Altun, M., Ekenel, M., Serilmez, M., Duranyildiz, D., Bavbek, S., Basaran, M., 2015. Diagnostic value of serum M30 and M65 in patients with nasopharyngeal carcinoma. Tumour biology : the journal of the International Society for Oncodevelopmental Biology and Medicine 36, 1039–1044.

Shen, L., Shao, N., Liu, X., Nestler, E., 2014. ngs.plot: quick mining and visualization of next-generation sequencing data by integrating genomic databases. BMC Genomics 15, 284.

Waltari, E., Jia, M., Jiang, C.S., Lu, H., Huang, J., Fernandez, C., Finzi, A., Kaufmann, D.E., Markowitz, M., Tsuji, M., Wu, X., 2018. 5′ rapid amplification of cDNA ends and Illumina MiSeq reveals B cell receptor features in healthy adults, adults with chronic HIV-1 infection, cord blood, and humanized mice. Front. Immunol. 9, 628.

Wu, J., Jia, S., Wang, C., Zhang, W., Liu, S., Zeng, X., Mai, H., Yuan, X., Du, Y., Wang, X., Hong, X., Li, X., Wen, F., Xu, X., Pan, J., Li, C., Liu, X., 2016. Minimal residual disease detection and evolved IGH clones analysis in acute B lymphoblastic leukemia using IGH deep sequencing. Front. Immunol. 7, 403.

Zhang, W., Du, Y., Su, Z., Wang, C., Zeng, X., Zhang, R., Hong, X., Nie, C., Wu, J., Cao, H., Xu, X., Liu, X., 2015. IMonitor: a robust pipeline for TCR and BCR repertoire analysis. Genetics 201, 459–472.

Zhu, J., Ofek, G., Yang, Y., Zhang, B., Louder, M.K., Lu, G., McKee, K., Pancera, M., Skinner, J., Zhang, Z., Parks, R., Eudailey, J., Lloyd, K.E., Blinn, J., Alam, S.M., Haynes, B.F., Simek, M., Burton, D.R., Koff, W.C., Program, N.C.S., Mullikin, J.C., Mascola, J.R., Shapiro, L., Kwong, P.D., 2013. Mining the antibodyome for HIV-1-neutralizing antibodies with next-generation sequencing and phylogenetic pairing of heavy/light chains. Proc. Natl. Acad. Sci. U. S. A. 110, 6470–6475.